Spintronic terahertz emitters exploiting uniaxial magnetic anisotropy for field-free emission and polarization control

DOI:
10.1063/5.0087282

Document Version
Accepted author manuscript

Spintronic terahertz emitters exploiting uniaxial magnetic anisotropy for field-free emission and polarization control

S. M. Hewett,[1,2,a)] C. Bull,[1,2] A. M. Shorrock,[2,b)] C.-H. Lin,[1,2] R. Ji,[1,2] M. T. Hibberd,[2,3] T. Thomson,[1] P. W. Nutter,[1] and D. M. Graham[2,3]

[1)] *Nano Engineering and Spintronic Technologies Group, Department of Computer Science, The University of Manchester, Oxford Road, Manchester M13 9PL, United Kingdom*

[2)] *Department of Physics and Astronomy & Photon Science Institute, The University of Manchester, Oxford Road, Manchester M13 9PL, United Kingdom*

[3)] *The Cockcroft Institute, Sci-Tech Daresbury, Keckwick Lane, Daresbury, Warrington WA4 4AD, United Kingdom*

(Dated: 7 March 2022)

We explore the terahertz (THz) emission from CoFeB/Pt spintronic structures in the below-magnetic-saturation regime and reveal an orientation dependence in the emission, arising from in-plane uniaxial magnetic anisotropy (UMA) in the ferromagnetic layer. Maximizing the UMA during the film deposition process and aligning the applied magnetic field with the easy axis of the structure, allows the THz emission to reach saturation under weaker applied fields. In addition, the THz emission amplitude remains at saturation levels when the applied field is removed. The development of CoFeB/Pt spintronic structures that can emit broadband THz pulses without the need for an applied magnetic field is beneficial to THz magneto-optical spectroscopy and facilitates the production of large-area spintronic emitters. Furthermore, by aligning the applied field along the hard axis of the structure, the linear polarization plane of the emitted THz radiation can be manipulated by changing the magnitude of the applied field. We therefore demonstrate THz polarization control without the need for mechanical rotation of external magnets.

[a)] Electronic mail: simmone.hewett@manchester.ac.uk

[b)] Present Address: QMC Instruments Ltd, School of Physics and Astronomy, Cardiff University, The Parade, Cardiff CF24 3AA, United Kingdom

Spintronic structures, consisting of thin multilayers of ferromagnetic (FM)/ non-magnetic (NM) materials, can produce single-cycle pulses of terahertz (THz) radiation when photo-excited by low-energy (nJ-level) femtosecond laser pulses. Current understanding of the emission process has been discussed in detail elsewhere.[1] THz emission is reported to result from the inverse spin-Hall effect (ISHE)[2] as a result of an injection of photo-driven spin current from the FM to the NM layer,[3] arising from the same force that drives ultrafast laser-driven demagnetization in FM thin films.[4] Spintronic structures have emerged as competitive sources of gap-free ultrabroadband THz frequency radiation, having demonstrated $300\,\mathrm{kV\,cm^{-1}}$ peak electric field strengths,[5] and gap-free 30 THz bandwidths.[6] The amplitude of the THz radiation emitted by spintronic structures has been shown to follow the magnetization $\boldsymbol{M}$ of the FM layer under the influence of an external magnetic field.[7,8] Typically, fields above 10 mT are used to ensure magnetic saturation of the FM layer in the plane of the structure, maximizing the amplitude of the emitted THz radiation.[6,7,9] In addition to controlling the amplitude of the emission, the direction of $\boldsymbol{M}$ also determines the direction of the plane of polarization of the emitted THz radiation,[6,7,10] which lies perpendicular to the direction of $\boldsymbol{M}$. The direct link observed between the magnetic response of spintronic structures and the resulting THz emission enables the creation of devices in which the THz amplitude and polarization are controlled at source through careful magnetic manipulation of the FM layer. Work has recently emerged on the use of time-dependent magnetic fields,[11] and FM layers engineered from anisotropic heterostructures,[12] to modulate the direction of the electric field of linearly polarized THz pulses. Spintronic structures within shaped magnetic fields[13,14] have also been used to generate the varied polarization profiles required by different technological applications.

A widely studied spintronic material system is CoFeB/Pt[1], which has been shown to offer optimum THz emission from this type of emitter.[6] Magnetic characterization of FM thin films has shown CoFeB to have in-plane uniaxial magnetic anisotropy (UMA) with orthogonal easy and hard magnetization axes.[15,16] While THz emission studies have noted the existence of in-plane magnetic anisotropy in the FM layers,[6,11] it is not usually evident in the THz emission from spintronic structures due to their operation within a saturating externally applied magnetic field. The potential for exploitation of the inherent UMA in easily fabricated spintronic bilayers has hence not been fully investigated.

In this Letter, we explore the THz emission from CoFeB/Pt bilayer spintronic structures

when the FM layer is at magnetic saturation, $\boldsymbol{M}_{\mathrm{S}}$, under an externally applied magnetic field, and subsequent remanent magnetization $\boldsymbol{M}_{\mathrm{R}}$, when the applied field is removed. We show that the remanence (zero field) THz emission is strongly dependent on the azimuthal orientation of the spintronic structure, relative to the initial direction of the applied external magnetic field, due to the existence of UMA in the FM layer. Enhancing the UMA, achieved here through manipulation of the deposition conditions, allows for the realization of a CoFeB/Pt spintronic structure that can operate as a field-free ultrabroadband THz emitter. When initially magnetized along an easy axis (EA), the field-free emitter maintains 98% of the THz signal amplitude observed under a saturating applied magnetic field, and shows no deterioration under a high photo-excitation fluence. Furthermore, exploiting the UMA by applying an external magnetic field along the hard axis (HA), results in the rotation of the THz polarization as the applied field is removed, due to an apparent rotation of the magnetic moment of the FM layer back towards the EA.

Our bilayers consist of a nominally 2.5 nm-thick $Co_{20}Fe_{60}B_{20}$ layer capped by 3 nm of platinum, deposited onto double-side polished fused silica substrates using DC-magnetron sputtering, under field-free conditions and a working gas pressure below 5×10^{-8} Torr. Layer thicknesses were determined using x-ray reflectivity (XRR) measurements, presented in supplementary material. In-plane UMA in FM films can arise as a result of oblique deposition, with the degree of UMA influenced by the rate of rotation of the sample holder during the deposition. Reduced anisotropy is reported with faster rotation of the holder, and for samples placed closer to its center to increase the angle of incident flux.[17,18] To influence the UMA in our fabricated spintronic structures, four CoFeB/Pt bilayers were deposited using rotation rates of either 0 or 9.4 rpm (maximum available rate). At each rotation rate, one sample was deposited with the substrate placed centrally (CoFeB target angle of 51.8° to the sample normal), and a second with the substrate at the edge of the sample holder (3.5 cm away from the central position, corresponding to a CoFeB target angle of 49.9°) to provide a small variation in the incident atomic flux angle.

To remove the influence of any edge effects on the anisotropy,[19] circular 8 mm diameter discs were cut from the deposited samples for magnetic and THz characterization. The four samples were designated: emitter A (9.4 rpm, center position), emitter B (9.4 rpm, edge position), emitter C (0 rpm, center), and emitter D (0 rpm, edge). These spintronic structures were held in a rotation mount between the poles of an electromagnet, powered

by a stabilized bi-polar DC supply, with the magnetic field applied along the plane of the structure. The applied magnetic field at the emitter position was measured using a Hall probe. The spintronic structures were excited by 100 fs laser pulses from a Ti:sapphire regenerative amplifier with 800 nm central wavelength and a repetition rate of 1 kHz. The laser pulses were split using a 90:10 beam splitter into pump and probe beams. The pump beam was at normal incidence to the bilayer structures with a fluence of 1.6 mJ cm^{-2}. The emitted THz radiation was focused onto a 1 mm thick (110)-cut ZnTe electro-optic detection crystal using a gold-coated 90° off-axis parabolic mirror and detected using standard electro-optic sampling techniques.[20] The residual pump beam emerging from the spintronic structure was blocked by an 800 nm filter. All measurements were performed in a relative humidity of 40%.

THz waveforms from all four emitters, shown in Fig. 1 (a), confirm that the deposition parameters have little effect on the saturation emission from the spintronic bilayers, with all four emitters producing identical waveforms with similar amplitudes. However, THz emission from remanent magnetization reveals a different degree of anisotropy for the different emitters. In this experiment, a uniform field of 40 mT, sufficient to saturate the FM layer, was applied in the plane of the structure, as shown in the insert to Fig. 1 (b), and the peak amplitude of the resulting horizontally polarized THz electric field (THz_S) was measured. The external magnetic field was then removed and the amplitude of the peak THz electric field emitted at remanence (THz_R) was measured. The measurements of THz_S and THz_R were repeated at 10° intervals for a full 360° azimuthal rotation of each emitter about the surface normal. The results for emitter A, which was found, as expected, to exhibit the least well-defined UMA, are shown in Fig.1 (b). At saturation, the THz emission is independent of azimuthal angle, however at remanence, uniaxial in-plane anisotropy is evident. With the emitter at a nominal azimuthal angle of 0°, THz_R retains 87% of the amplitude of THz_S. In this orientation, the in-plane EA of the structure is parallel to the applied magnetic field. With the emitter azimuthally rotated through 90°, the in-plane HA becomes aligned with the applied field and THz_R falls to 45% of THz_S.

Fig. 2 (a) and (b), show THz_R normalized to THz_S for all four emitters. The results confirm that the anisotropy is enhanced by having the substrate stationary during the deposition, and is more sharply defined in samples deposited at both rotation speeds for edge compared to central position of the substrate during the deposition. We attribute below zero

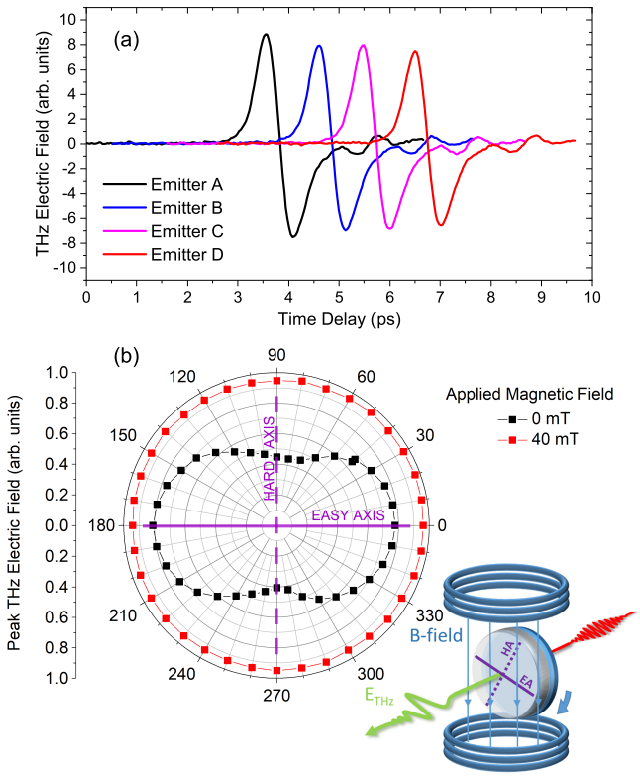

FIG. 1. (a) THz waveforms (horizontally offset for clarity) from CoFeB/Pt spintronic emitters A, B, C and D under a saturating applied magnetic field of 40 mT. (b) Peak THz electric field amplitude from emitter A as a function of azimuthal rotation about the surface normal, under saturation (red line) and from remanent magnetization (black line). The easy axis is defined as 0°. The inset shows the orientation of the fixed magnetic field with respect to the plane of the spintronic emitter, and the resulting horizontally polarized THz emission.

values for emitter C when aligned along the hard axis to thermal fluctuations in the low value of $\boldsymbol{M}$. Most interestingly, with alignment of the applied field along the EA, both edge deposited structures (emitters B and D) exhibit $\mathrm{THz_R/THz_S}$ approaching unity, realizing field-free spintronic emitters with no loss of THz signal. THz emission from spintronic structures at remanence has been previously reported,[8,21,22] but with significantly reduced electric field amplitudes when compared to emission at saturation. Kampfrath *et al.*[21] reported THz emission from an Fe/Au bilayer, with emission at remanence falling to 53% of the amplitude seen with an in-plane saturating magnetic field. Emission from ferrimagnetic $\mathrm{Tb}_x\mathrm{Fe}_{1-x}$/Pt structures with varying Tb content was reported at remanence with 63% of the THz ampli-

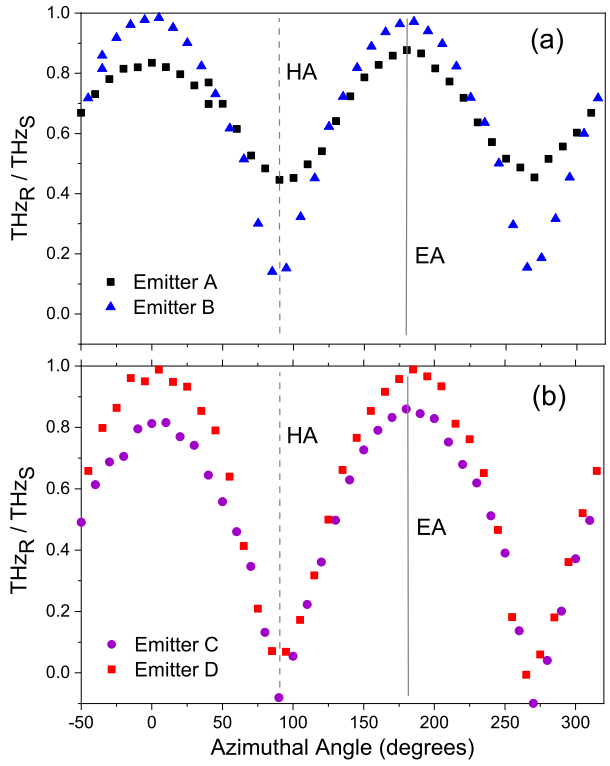

FIG. 2. Dependence on azimuthal orientation of the peak THz electric field amplitude from remanent magnetization (THz_R) normalized to peak amplitude with magnetic saturation (THz_S) for (a) emitters A (center deposited) and B (edge deposited), deposited under rotation, and (b) emitters C (center) and D (edge), deposited without rotation.

tude seen under saturation.[8] More recently, Guo *et al.* reported THz emission at remanence from a W/CoFeB/Pt trilayer deposited on glass, though no comparison to emission at saturation was made.[22] Our results show that exploiting UMA in spintronic structures provides a simple method to maximize the amplitude of the field-free THz emission.

Further measurements were carried out using emitter D, which exhibited the most well-defined UMA. THz emission as a function of applied magnetic field was measured for alignment of the field with the EA and the HA of the structure. For both orientations, the applied magnetic field was cycled between $\pm 40\,\mathrm{mT}$ and the maximum amplitude of the THz signal was recorded at 1 mT intervals, reducing to 0.25 mT intervals at field strengths below $\pm 2\,\mathrm{mT}$. The resulting hysteresis behavior is shown in Fig. 3(a). EA alignment produces a characteristically square shaped hysteresis loop, demonstrating the abrupt reversal of magnetic domains. The HA loop shows a more gradual reversal of the magnetization and

approaches the diagonal line characteristic of an idealized HA in a uniaxial material. The coercivity of around 1 mT is found to be independent of the applied field angle. However, the magnetic field strength required to achieve saturation is orientation dependent, with the structure saturating at around 1 mT along the EA but requiring over 8 mT to achieve saturation along the HA. The corresponding vibrating sample magnetometry (VSM) data, showing the magnetization of the structure as a function of in-plane applied magnetic field, is provided in Fig. 3(b). It should be noted that VSM measures the magnetic response across the entire structure, whereas the THz emission is localized to the photoexcited region. Nevertheless, the loops in Fig. 3(a) and (b) are well-matched, showing the inherent

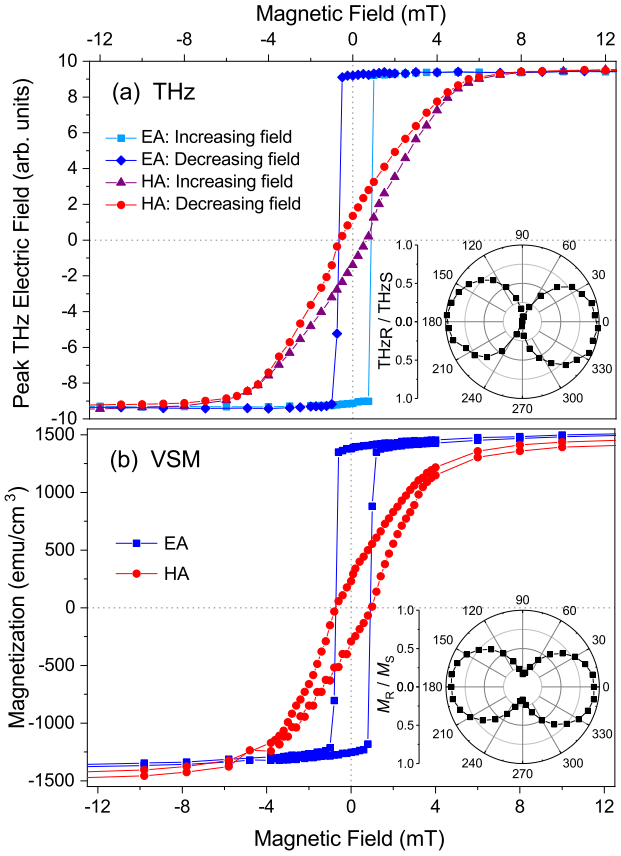

FIG. 3. (a) THz electric field amplitude as a function of in-plane external magnetic field, with the magnetizing field aligned parallel to the EA or the HA. (b) Corresponding VSM hysteresis loops for the matched emitter orientations. Inserts to (a) and (b) show the azimuthal dependence of the ratio of the peak THz electric field at 0 mT ($\mathrm{THz_R}$) to that with 40 mT applied field ($\mathrm{THz_S}$), and the corresponding ratio of residual magnetization M_R to saturation magnetization M_S.

link between the magnetization of a spintronic structure and the THz emission behavior. This is further evidenced in the inserts to each graph, which show the azimuthal-dependence of the ratio of THz_R to THz_S, and the corresponding ratio of the magnetizations M_R/M_S.

The stability of the field-free THz emission amplitude over time was tested, under an increased 2 mJ cm^{-2} fluence. A THz scan of emitter D was performed under a saturating 40 mT field applied along the EA. The magnetic field was then removed and a new field-free THz scan was recorded. Under continuous laser excitation over a 3 hour period and with the emitter remaining free of any applied field, further THz waveforms were recorded at 30 minute intervals. The results, presented in Fig. 4 (a), show that the field-free THz emission shows no observable deterioration over time under continuous excitation. The spectral bandwidths of the saturated and field-free THz emission, shown in Fig. 4 (b), are also identical. Here, the bandwidth was limited by the 0.5 mm thick ZnTe crystal and the 100 fs laser pulse duration used in this experiment. However, the structure is capable of ultrabroadband THz emission when pumped with shorter duration pulses (see supplementary material for THz amplitude spectra generated using sub-20 fs laser pulses and a 0.1 mm thick ZnTe detection crystal).

Field-free THz emission has recently been reported from synthetic antiferromagnetic (SAF) spintronic structures,[23,24], which consist of exchange-coupled ferromagnetic layers separated by metallic or dielectric spacer layers. However, these structures are challenging to fabricate as they require the growth of very smooth multilayers of precise thickness, due to the strong dependence of the interlayer exchange coupling on the thickness of the spacer layer (SL).[25,26] Furthermore, it has been shown that the THz emission generated from SAF structures is limited by the total thickness of the structure.[23] It is challenging to reduce this below ≈10 nm due to the minimum number of layers, $NM_1/FM_1/SL/FM_2/NM_2$, required for the SAF structure to function as a field-free spintronic THz emitter.[24] Exploiting UMA in easily fabricated spintronic bilayers, provides a cost-effective alternative for the generation of high amplitude, stable, field-free THz emission.

In addition to field-free emission, exploitation of UMA in simple spintronic bilayers may find particular application in THz polarization control. In a recent study by Khusyainov *et al.*,[32] a strong in-plane UMA was induced in a multi-stack spintronic structure in order to manipulate the THz wave polarization through the variation of the magnitude of a DC magnetic field with fixed direction. The structure contained seven layers of alternating $TbCo_2$

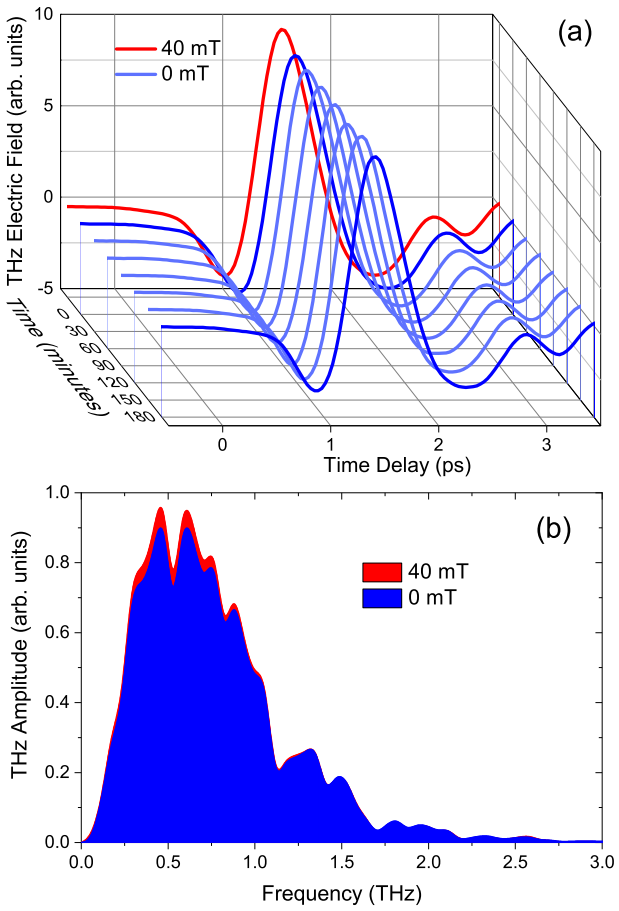

FIG. 4. (a) THz waveforms from emitter D aligned along the easy axis from an initial saturating applied field of 40 mT and with the field subsequently removed. Field-free THz waveforms are shown that were recorded every 30 minutes over a period of 3 hours. (b) Corresponding THz amplitude spectra from saturation (40 mT) and initial remanent (0 mT) magnetization.

and FeCo, deposited on glass under an applied magnetic field and capped with Ru, creating a stack of total thickness 30.4 nm. Given the reduction in THz signal amplitude known to result from increasing metal stack thickness,[6] enhancing UMA in simple bilayer structures may provide a field-sensitive alternative and more readily allow for thickness optimization of the structures. To test this hypothesis, a polarization resolved detection setup utilizing a 0.5 mm thick (111)-cut ZnTe crystal,[33] was used to measure the THz radiation emitted by our spintronic structures when initially magnetized by a 40 mT field applied in-plane along their HA (y-direction), and with the field subsequently removed. Fig. 5 (a) and (b) show the THz electric field amplitudes, together with their E_x and E_y components, of emitter

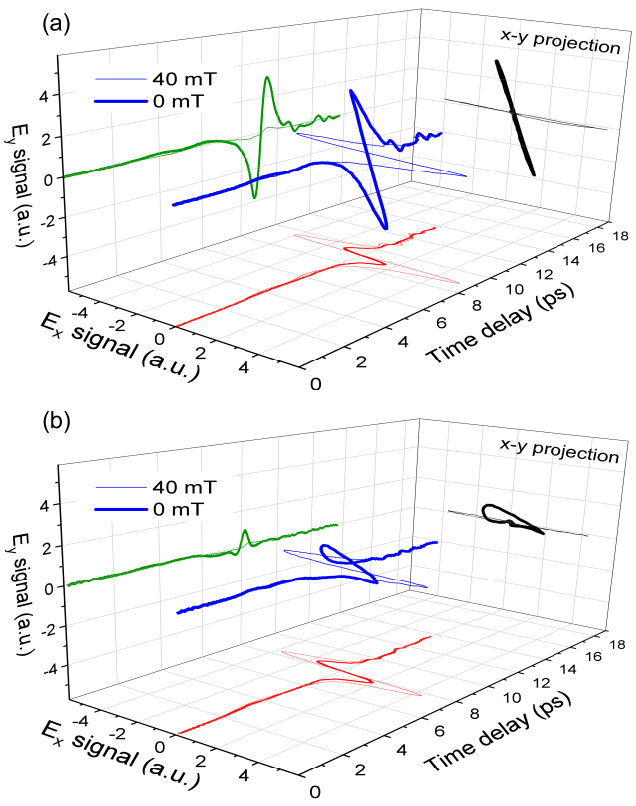

FIG. 5. THz waveforms (blue), and their constituent E_x (red) and E_y (green) components, for (a) emitter D (most well-defined UMA), and (b) emitter A (least-defined UMA). Thin lines show the waveforms obtained under a saturating 40 mT field, applied in the y-direction parallel to the HA; thick lines show the result of reducing this field to zero.

D with the greatest UMA (a) and emitter A with the least UMA (b). In both structures, under saturation, the THz polarization is aligned with the x-direction. With the applied field removed, the linear polarization of emitter D, with well-defined UMA, is seen to rotate towards the y-direction (Fig. 5(a)) as the magnetization rotates back towards the EA of the structure. The exploitation of a well-defined UMA in the FM layer thus provides the potential for polarization control without the need for mechanical rotation of external magnets. In contrast, for emitter A, which exhibits a less defined UMA, shown in Fig. 5(b), reducing the applied field to zero results in a more complex behavior of the magnetization, and a loss of linear polarization.

In conclusion, we have demonstrated that THz emission from spintronic structures is sensitive to the inherent in-plane UMA in the FM layer. With the external magnetic field

aligned along the EA of the structure, the resultant peak THz emission is shown to be achieved at lower applied magnetic field than with HA alignment. This orientation dependence is a potentially important consideration in low-field and field-switching schemes. THz emission from CoFeB/Pt bilayers at remanence, is found to depend on the azimuthal orientation of the structures with respect to the applied field. The UMA can be exploited to allow the structure to act as a field-free THz emitter, with the emission showing no observable deterioration over time. The ability to operate spintronic emitters under field-free conditions, with no amplitude reduction, also removes their one disadvantage in comparison to photoconductive antenna and non-linear crystal THz sources. This could widen their practical application, for example in THz magneto-optical spectroscopy of field sensitive materials such as ferrofluids,[27–29] metasurfaces,[30] and magnetic tunnel junctions.[31] The removal of the requirement for operation within a magnetic field could also facilitate the scaling up of spintronic structures to produce large-area, high-field THz emitters. Applying a varying magnetic field parallel to the HA of a spintronic structure with enhanced UMA has also been shown to provide effective THz polarization control, enabling rotation of the plane of polarization without mechanical rotation of the magnets. Exploitation of UMA in spintronic structures may prove a key step in the development of zero-field and low-field applications, and provide enhanced control in field shaping schemes that show promise for all-magnetic control of THz polarization profiles.

See supplementary material for x-ray reflectivity measurements, additional VSM data, and broadband THz amplitude spectra generated using sub-20 fs duration pump pulses.

ACKNOWLEDGMENTS

This work was supported by the United Kingdom Engineering and Physical Sciences Research Council [Grant No. EP/S033688/1]. We also wish to acknowledge the Ph.D. scholarship support for R. Ji by the China Scholarship Council (NSCIS Grant No. 201906120039).

DATA AVAILABILITY

The data associated with the paper are openly available from the Zenodo data repository at: http://dx.doi.org/xx.xxxxx/xxxxxxxxxxxx.

REFERENCES

[1]C. Bull, S. M. Hewett, R. Ji, C.-H. Lin, T. Thomson, D. M. Graham, and P. W.Nutter, APL Mater. **9**,090701 (2021).

[2]E. Saitoh, M. Ueda, H. Miyajima, and G. Tatara, Appl. Phys. Lett. **88**, 182509 (2006).

[3]A. G. Aronov, JETP Lett. **24**, 32 (1976).

[4]S. Rouzegar, L. Brandt, L. Nádvorník, D. Reiss, A. Chekhov, O. Gueckstock, C. In, M. Wolf, T. Seifert, P. Brouwer, G. Woltersdorf, and T. Kampfrath, Cond-Mat.Mes-Hall , arXiv:2103.11710 (2021).

[5]T. Seifert, S. Jaiswal, M. Sajadi, G. Jakob, S. Winnerl, M. Wolf, M. Kläui, and T. Kampfrath, Appl. Phys. Lett. **110**, 252402 (2017).

[6]T. Seifert, S. Jaiswal, U. Martens, J. Hannegan, L. Braun, P. Maldonado, F. Freimuth, A. Kronenberg, J. Henrizi, I. Radu, E. Beaurepaire, Y. Mokrousov, P. M. Oppeneer, M. Jourdan, G. Jakob, D. Turchinovich, L. M. Hayden, M. Wolf, M. Münzenberg, M. Kläui, and T. Kampfrath, Nat. Photonics **10**, 483 (2016).

[7]R. Adam, G. Chen, D. E. Bürgler, T. Shou, I. Komissarov, S. Heidtfeld, H. Hardtdegen, M. Mikulics, C. M. Schneider, and R. Sobolewski, Appl. Phys. Lett. **114**, 212405 (2019).

[8]R. Schneider, M. Fix, R. Heming, S. Michaelis de Vasconcellos, M. Albrecht, and R. Bratschitsch, ACS Photonics **5**, 3936 and suppl. mat. (2018).

[9]D. Yang, J. Liang, C. Zhou, L. Sun, R. Zheng, S. Luo, Y. Wu, and J. Qi, Adv. Opt. Mater. **4**, 1944 (2016).

[10]G. Li, R. V. Mikhaylovskiy, K. A. Grishunin, J. D. Costa, Th. Rasing, and A. V. Kimel, J. Phys. D: Appl. Phys. **51**, 134001 (2018).

[11]O. Gueckstock, L. Nádvorník, T. S. Seifert, M. Borchert, G. Jakob, G. Schmidt, G. Woltersdorf, M. Kläui, M. Wolf, and T. Kampfrath, Optica **8**, 1013 (2021).

[12]P. Koleják, G. Lezier, K. Postava, J.-F. Lampin, N. Tiercelin, and M. Vanwolleghem, arXiv:2111.07118v1 [physics.optics] (2021).

[13]M. T. Hibberd, D. S. Lake, N. A. B. Johansson, T. Thomson, S. P. Jamison, and D. M. Graham, Appl. Phys. Lett. **114**, 031101 (2019).

[14]H. Niwa, N. Yoshikawa, M. Kawaguchi, M. Hayashi and R. Shimano, Opt. Express **29**, 13331 (2021).

[15]A. T. Hindmarch, A. W. Rushforth, R. P. Campion, C. H. Marrows, and B. L. Gallagher, Phys. Rev. B **83**, 212404 (2011).

[16]Z. Hao, L. Yuan-Yuan, Y. Mei-Yin, Z. Bao, Y. Guang, W. Shou-Guo, and W. Kai-You, Chinese Phys. B **24**, 077501 (2015).

[17]T. P. Bertelli, T. E. P. Bueno, A. C. Krohling, B. C. Silva, R. L. Rodríguez-Suárez, V. P. Nascimento, R. Paniago, K. Krambrock, C. Larica, and E. C. Passamani, J. Magn. Magn. Mater **426**, 636 (2017).

[18]J. B. S. Mendes, L. H. Vilela-Leão, S. Rezende, and A. Azevedo, IEEE Trans. Magn. **46**, 2293 (2010).

[19]B. A. Belyaev, A. V. Izotov, G. V. Skomorokhov, and P. N. Solovev, Mater. Res. Express, **6**, 11 (2019).

[20]Q. Wu, and X.-C. Zhang, Appl. Phys. Lett. **67**, 3523 (1995).

[21]T. Kampfrath, M. Battiato, P. Maldonado, G. Eilers, J. Nötzold, S. Mährlein, V. Zbarsky, F. Freimuth, Y. Mokrousov, S. Blügel, M. Wolf, I. Radu, P. M. Oppeneer, and M. Münzenberg, Nat. Nanotechnol. **8**, 256, suppl. mat. (2013).

[22]F. Guo, C. Pandey, C. Wang, T. Nie, L. Wen, W. Zhao, J. Miao, L. Wang, and X. Wu, OSA Continuum **3**, 893 (2020).

[23]Q. Zhang, Y. Yang, Z. Luo, Y. Xu, R. Nie, X. Zhang, and Y. Wu, Phys. Rev. Applied **13**, 054016 (2020).

[24]Y. Ogasawara, Y. Sasaki, S. Iihama, A. Kamimaki, K. Z. Suzuki and S. Mizukami, Appl. Phys. Express **13**, 063001 (2020).

[25]S. S. Parkin and D. Mauri, Phys. Rev. B **44**, 7131 (1991).

[26]H. J. Waring, N. A. B. Johansson, I. J. Vera-Marun, and T. Thomson, Phys. Rev. Appl. **13**, 034035 (2020).

[27]M. Shalaby, M. Peccianti, Y. Ozturk, M. Clerici, I. Al-Naib, L. Razzari, T. Ozaki, A. Mazhorova, M. Skorobogatiy, and R. Morandotti, Appl. Phys. Lett. **100**, 241107 (2012).

[28]F. Fan, S. Chen, W. Lin, Y.-P. Miao, S.-J. Chang, B. Liu, X.-H. Wang, and L. Lin, Appl. Phys. Lett. **103**, 161115 (2013).

[29]M. Shalaby, M. Peccianti, Y. Ozturk, I. Al-Naib, C. P. Hauri, and R. Morandotti, Appl. Phys. Lett. **105**, 151108 (2014).

[30]T.-F. Li, Y.-L. Li, Z.-Y. Zhang, Q.-H. Yang, F. Fan, Q.-Y. Wen, and S.-J. Chang Appl. Phys. Lett. **116**, 251102 (2020).

[31]Z. Jin, J. Li, W. Zhang, C. Guo, C. Wan, X. Han, Z. Cheng, C. Zhang, A. V. Balakin, A. P. Shkurinov, Y. Peng, G. Ma, Y. Zhu, J. Yao, and S. Zhuang, Phys. Rev. Applied **14**, 014032 (2020).

[32]D. Khusyainov, S. Ovcharenko, M. Gaponov, A. Buryakov, A. Klimov, N. Tiercelin, P. Pernod, V. Nozdrin, E. Mishina, A. Sigov, and V. Preobrazhensky, Sci. Reports **11**, 697 (2021).

[33]N. C. J. van der Valk, W. A. M. van der Marel, and P. C. M. Planken, Opt. Lett. **30**, 2802 (2005).